bioRxiv preprint first posted online Sep. 30, 2019; doi: http://dx.doi.org/10.1101/787192. The copyright holder for this preprint (which was not peer-reviewed) is the author/funder, who has granted bioRxiv a license to display the preprint in perpetuity. It is made available under a CC-BY-NC-ND 4.0 International license.

Developmental onset of enduring long-term potentiation in mouse hippocampus

Olga I. Ostrovskaya[1], Guan Cao[1]*, Cagla Eroglu[2,3,4], Kristen M. Harris[1]

1 Center for Learning and Memory
Department of Neuroscience
The University of Texas at Austin
Austin, Texas 78712

2 Department of Cell Biology
3 Department of Neurobiology
4 Regeneration Next Initiative
Duke University Medical Center
Durham, NC 27710

* Olga I. Ostrovskaya and Guan Cao are co-first authors

Corresponding Author:
Kristen M. Harris, PhD
The University of Texas at Austin
Center for Learning and Memory
1 University Station C7000
Austin, TX 78712-0805
kharris@mail.clm.utexas.edu
512.232.3968

Running Title: Developmental onset of L-LTP in mouse hippocampus

bioRxiv preprint first posted online Sep. 30, 2019; doi: http://dx.doi.org/10.1101/787192. The copyright holder for this preprint (which was not peer-reviewed) is the author/funder, who has granted bioRxiv a license to display the preprint in perpetuity. It is made available under a CC-BY-NC-ND 4.0 International license.

KEY POINTS SUMMARY (150 words max, currently 150, 5 bullets)

- Saturating theta-burst stimulation (TBS) was used to discern the developmental age when short-term potentiation (STP) lasting 1 hour and late long-term potentiation (L-LTP) lasting ≥3 hr are first expressed in mouse hippocampus.
- Four mouse strains were compared—C57BL/6 and *Fmr1*$^{-/y}$ on C57BL/6 background and 129SVE and *Hevin*$^{-/-}$ (*Sparcl1*$^{-/-}$) on 129SVE background—because both gene manipulations alter dendritic spines.
- In all four strains, STP onset was gradual, first occurring between postnatal days (P) 10-28, while reliable L-LTP emerged in C57BL/6 and *Fmr1*$^{-/y}$ at P35, and in 129SVE and *Hevin*$^{-/-}$ (*Sparcl1*$^{-/-}$) at P28.
- In contrast to rat hippocampus, multiple episodes of TBS did not alter the onset age of L-LTP in mouse hippocampus.
- The L-LTP onset age in rat hippocampus is P12, coincident with the first appearance of dendritic spines. Others report spine appearance by P24 in mouse hippocampus, suggesting spines may be necessary but not sufficient for L-LTP.

ABSTRACT (250 words max, currently 243)

Analysis of long-term potentiation (LTP) provides a powerful window into cellular mechanisms of learning and memory. Prior work shows late LTP (L-LTP), lasting three or more hours, first occurs at postnatal day 12 (P12) in Long-Evans rat hippocampus. The goal of the current work was to determine the developmental onset of L-LTP in mouse hippocampus as a basis for comparing potential effects of key genetic manipulations known to affect dendritic spine structure. Four mouse strains were tested. Both C57BL/6 and *Fmr1*$^{-/y}$ mice on the C57BL/6 background began to show reliable L-LTP at P35. In contrast, both 129SVE wild type and *Hevin*$^{-/-}$ (*Sparcl1*$^{-/-}$) on the 129SVE background first showed reliable L-LTP at P28. All strains showed a gradual progression between P10 to P28 in success rate for short-term potentiation (STP), which lasts one hour or less. At P10 in rats, two episodes of TBS result in L-LTP when the time between episodes was ≥ 90 minutes. In mice, multiple bouts of TBS at various inter-bout intervals did not advance the onset age of L-LTP. Prior work in rats showed the onset of L-LTP at P12 coincided with the first formation of dendritic spines. In contrast, hippocampal dendritic spines are present by P24 in C57BL/6 mice, well before the onset age for L-LTP. These species-dependent findings suggest that dendritic spines may be necessary but not sufficient for L-LTP.

bioRxiv preprint first posted online Sep. 30, 2019; doi: http://dx.doi.org/10.1101/787192. The copyright holder for this preprint (which was not peer-reviewed) is the author/funder, who has granted bioRxiv a license to display the preprint in perpetuity. It is made available under a CC-BY-NC-ND 4.0 International license.

INTRODUCTION

Long-term potentiation (LTP) is a cellular mechanism of learning and memory. Knowing the developmental profile for LTP provides a basis for investigating developmental abnormalities leading to intellectual disabilities and other neurodevelopmental disorders. Our previous work on Long-Evans rats revealed that theta-burst stimulation (TBS) reversed test pulse depression at postnatal day 8 (P8) through P11, but no potentiation was produced above the initial naïve response. In contrast, at P12 TBS reliably induced enduring LTP lasting more than 3 hours, i.e., late LTP (L-LTP). When multiple episodes of TBS were delivered, L-LTP resulted at P10-P11. In rats this developmental onset of LTP is coincident with the emergence of dendritic spines, supporting the hypothesis that dendritic spines are necessary for LTP during development (Cao and Harris, 2012; Fiala et al., 1998; Kirov et al., 2004).

Mice are a widely used model system to test the effects of genetic manipulations on normal behavior and physiology (Ellenbroek and Youn, 2016; Homberg et al., 2017). Little is known about the developmental profile of synaptic plasticity in mice. Two commonly used wild type mouse strains, C57BL/6 and 129SVE, were chosen together with *Fmr1*$^{-/y}$ and *Hevin*$^{-/-}$ (*Sparcl1*$^{-/-}$), both of which are known for aberrations in synaptic plasticity and development. *Fmr1*$^{-/y}$ on the C57BL/6 background is a common model of Fragile X syndrome (FXS) for mental retardation and autism. The cause of FXS is the mutation preventing the synthesis of FMRP, an RNA-binding protein selectively expressed in neurons and responsible for mRNA transport and local protein synthesis in dendrites. Alterations in dendritic spines along with disruptions in plasticity are characteristic of FXS (He and Portera-Cailliau, 2013; Pfeiffer and Huber, 2009). Hevin is a protein released by astrocytes and interneurons that is critical for synapse formation and rearrangement (Mongredien et al., 2019). The synaptogenic activity of Hevin promotes glutamatergic synapse maturation and refines cortical connectivity and plasticity (Risher et al., 2014; Singh et al., 2016), both of which are disrupted in *Hevin*$^{-/-}$ (*Sparcl1*$^{-/-}$) on the 129SVE background.

The effects of knocking out *Fmr1* or *Hevin* on the maturation of synaptic plasticity are unknown. We tested both mouse strains to determine the developmental onset age of L-LTP in response to TBS in hippocampal area CA1. The *Fmr1*$^{-/y}$ and *Hevin*$^{-/-}$ were similarly tested to determine whether these important mutations alter the developmental profile of LTP in the mouse. The outcomes provide new insights about species and strain differences in the maturation of LTP and raise questions about the role of dendritic spines.

MATERIALS AND METHODS

Ethical Approval. Procedures were approved by the University of Texas at Austin Institutional Animal Care and Use Committee and complied with all NIH requirements for the humane care and use of laboratory mice (protocol # AUP-2012-00127, AUP-2012-00056, and their successor protocols).

bioRxiv preprint first posted online Sep. 30, 2019; doi: http://dx.doi.org/10.1101/787192. The copyright holder for this preprint (which was not peer-reviewed) is the author/funder, who has granted bioRxiv a license to display the preprint in perpetuity. It is made available under a CC-BY-NC-ND 4.0 International license.

Animals. Breeding pairs of C57BL/6 (RRID:IMSR_JAX:000664) and *Fmr1*$^{-/y}$ (RRID:MGI:5703659) on this background were kindly donated by Dr. D. Brager (Center for Learning and Memory, University of Texas at Austin) who received the founder pair from Dr. K. Huber (University of Texas Southwestern). Breeding pairs of 129SVES6 mice were obtained from a supplier (Taconic, Rensselaer, NY; RRID:IMSR_TAC:129sve) and *Hevin*$^{-/-}$ (*Sparcl1*$^{-/-}$, allelic composition *Sparcl1*^{tm1Pmc}/*Sparcl1*^{tm1Pmc}, RRID:MGI:4454665) were on this background. We will be referring to this knock-out as *Hevin*$^{-/-}$. The generation of *Fmr1*$^{-/y}$ and *Hevin*$^{-/-}$ (*Sparcl1*$^{-/-}$) has been described before (1994; Barker et al., 2005)(McKinnon et al., 2000). Animals were co-housed and provided with food and water *ad libitum* on a 12 hr light-dark cycle. The experimental design was originally optimized for the *Fmr1*$^{-/y}$ mice, in which the males have the strongest phenotypes; hence, for the appropriate comparison with *Fmr1*$^{-/y}$ data, males were used for all of these experiments. The exact age of each animal was known; however, for ease of graphical presentation, animals were grouped as P10-13 (<2 wks), P13-17 (2 wks), P18-23 (3 wks), P26-31 (4 wks), and P32-37 (5 wks).

Slice preparation. Hippocampal slices were prepared from mouse pups at P8 to P38 as previously described (Bourne et al., 2007). Animals were decapitated under isoflurane anesthesia when appropriate (age older than P33). The brain was removed, and the left hippocampus was dissected out and rinsed with room temperature artificial cerebrospinal fluid (aCSF) containing (in mM) 117 NaCl, 5.3 KCl, 26 $NaHCO_3$, 1 NaH_2PO_4, 2.5 $CaCl_2$, 1.3 $MgSO_4$, and 10 glucose, pH 7.4, and bubbled with 95% O_2-5% CO_2. Four slices (400 μm thick) from the middle third of the hippocampus were cut at 70° transverse to the long axis on a tissue chopper (Stoelting, Wood Dale, IL) and transferred to four individual interface chambers in the Synchroslice system (Lohmann Research Equipment, Castrop-Rauxel, Germany). The slices were placed on a net at the liquid-gas interface between aCSF and humidified 95% O_2-5% CO_2 atmosphere held at 32-33°C. The entire dissection and slice preparation took 5-7 min. The slices recovered in the chambers for 3 hr before the recordings commenced.

Electrophysiology. The stimulation and data acquisition were obtained using the SynchroBrain software (Lohmann Research Equipment). A concentric bipolar stimulating electrode (FHC Inc., Bowdoin, ME) was positioned near the CA3 side, and a metal recording electrode (Thomas Recording, Geissen, Germany) was placed ~400 μm away from the stimulating electrode, also in the middle of CA1 *stratum radiatum*. Stimuli consisted of 200 μs biphasic current. An I/O curve was generated by measuring the slope (mV/ms) of the extracellular field excitatory postsynaptic potentials (fEPSPs) in response to increasing stimulus intensities (ranging from 100-500 μA). The I/O curve determined the 50% response that was used for the subsequent stimulation. The naïve fEPSP was the first response obtained at that 50% level upon completion of the I/O curve. The fEPSP slopes (mV/ms) were estimated by linear regression over the 0.2-0.4 ms interval in the middle section of the slope. This analysis time frame was kept constant for each slice throughout the recording. The stimulus intensity required to obtain ~1/2 maximal fEPSP slope was held constant for the duration of each experiment and applied every 2.5 min.

bioRxiv preprint first posted online Sep. 30, 2019; doi: http://dx.doi.org/10.1101/787192. The copyright holder for this preprint (which was not peer-reviewed) is the author/funder, who has granted bioRxiv a license to display the preprint in perpetuity. It is made available under a CC-BY-NC-ND 4.0 International license.

The various TBS paradigms are described in the figures and Results section. Briefly, the 8T TBS paradigm consisted of eight trains with 30 s intervals with each train containing 10 bursts at 5 Hz and each burst containing 4 pulses at 100 Hz. The 1T TBS paradigm consisted of one train of the same stimulation pattern. The fEPSP slope is expressed as a percentage of the naïve fEPSP or the averaged baseline response obtained 30 min before delivering the TBS paradigm as indicated in the Results and figures. Baseline responses were recorded for 60 min before the delivery of the TBS paradigm. Experiments within an age were grouped depending on the success of inducing potentiation with a threshold set at 120% of the naïve fEPSP slope.

Statistics. Statistical analyses were performed using Prism (GraphPad Software, Inc.; San Diego, CA). Data are presented throughout as the mean ± SEM. The minimal level of significance was set at $p<0.05$. The specific tests and the outcomes are indicated in the figure legends. Throughout the text, n refers to the number of slices. The total number of animals and slices of each cohort (genotype/age) is presented in Table 1.

RESULTS

Strain- and genotype-specific differences in developmental onset of STP and L-LTP.

Prior work in rats revealed that L-LTP has an abrupt developmental onset at P12 in response to saturating theta-burst stimulation (TBS) (Cao and Harris, 2014). The saturating protocol consists of eight trains of TBS (8T) and reliably produced L-LTP lasting ≥ 3 hr in the hippocampal area CA1 of adult C57BL/6 mice (7-9 wks old). *Saturating* means that additional episodes of TBS delivered at less than a 90 minute interval produce no additional LTP, i.e., they do not augment LTP. Here, we aimed to determine the age when 8T first elicits L-LTP in mouse hippocampal area CA1. Early during development, before P20 in rat hippocampus, baseline stimulation produces a marked depression of the fEPSPs, and high frequency tetanic stimulation (HFS) and TBS both can reverse the depression but produce no potentiation above the first naïve response (Abrahamsson et al., 2007, 2008; Xiao et al., 2004). To discern between the reversal of test pulse depression and LTP, all responses were normalized relative to the first naïve response. The LTP threshold was set at 120%. For each age, the number of experiments were tabulated where TBS failed (none) or succeeded in producing short-term potentiation lasting 1 hr (STP 1h) or L-LTP (LTP 3h). In mice, unlike rats, the onset for L-LTP occurred across weeks instead of days, hence the data were grouped by weeks, based on the relative frequency of slices showing L-LTP (Fig. 1-4). The *Before Onset* groups comprised ages where L-LTP was induced in 25% or less of tested slices. The *Onset* groups had 26-50% success rate among tested slices. The *After Onset* groups had L-LTP in more than 50% of tested slices.

Fig. 1-5

First, we tested mice from the C57BL/6 strain and *Fmr1*$^{-/y}$ on C57BL/6 background. By 2 weeks, all slices showed de-depression and about 16% of slices showed STP, but none had L-LTP for the C57BL/6 wild type mice (Fig. 1A1). By 3 weeks, 31% of slices from the *Fmr1*$^{-/y}$ mutant mice

bioRxiv preprint first posted online Sep. 30, 2019; doi: http://dx.doi.org/10.1101/787192. The copyright holder for this preprint (which was not peer-reviewed) is the author/funder, who has granted bioRxiv a license to display the preprint in perpetuity. It is made available under a CC-BY-NC-ND 4.0 International license.

showed STP and 7% showed L-LTP (Fig. 1B1). Between 3-4 weeks, 41% of slices produced STP and 26% produced L-LTP in the C57BL/6 wild type (Fig. 1A2); whereas, in the *Fmr1*$^{-/y}$ mutants, at 4 weeks 30% of slices produced STP and 40% produced L-LTP (Fig. 1B2). By 5 weeks, L-LTP was reliably produced in more than 50% of slices from both the C57BL/6 wild types and *Fmr1*$^{-/y}$ mutants (Fig. 1A3, 1B3). Figure 2 illustrates these findings on a weekly basis for each strain. These findings suggest a gradual onset for the production of STP and L-LTP in the C57BL/6 strain, an effect that was apparently delayed in *Fmr1*$^{-/y}$.

Next, we tested mice from the 129SVE strain and *Hevin*$^{-/-}$ on the 129SVE background. Before 2 weeks, all slices showed de-depression, one out of 10 slices showed minimal L-LTP in the 129SVE mice (Fig. 3A1), and one out of 11 slices showed subtle STP in *Hevin*$^{-/-}$ (Fig. 3B1), but most slices showed no potentiation. By 3 weeks, 38% of slices showed STP or L-LTP in the 129SVE mice (Fig. 3A2), contrasting with 33% of slices from *Hevin*$^{-/-}$ showing L-LTP a week earlier by 2 weeks (Fig. 3B2). By 4 weeks, 80% of slices showed L-LTP and 10% had STP in the 129SVE mice (Fig. 3A3). Figure 4 illustrates these findings on a weekly basis. Thus, reliable L-LTP occurred at 4 weeks in the 129SVE strain and even earlier, at 3 weeks, for *Hevin*$^{-/-}$.

Additional experiments demonstrated that 1T, 2T, and 8T produced L-LTP of the same magnitude and endurance at 4-5 weeks (Fig. 5). Hence, the 8T was adopted as a conservative approach consistent with the same paradigm that saturates L-LTP in adult rats and adult C57BL/6 mice (Abraham and Huggett, 1997; Cao and Harris, 2014; Kramar et al., 2012).

L-LTP onset was delayed in Fmr1$^{-/y}$ *and accelerated in Hevin*$^{-/-}$ *knockouts.*

Fig. 6

The probability of producing STP or L-LTP was compared across ages, strains, and genotypes (Fig. 6). The onset of STP appeared earliest in the *Hevin*$^{-/-}$ mice; however, this effect was not statistically significant, and all strains had $\geq$ 50% of slices showing STP by week 3 (Fig. 6A). The Onset and After Onset ages for L-LTP were significantly earlier at 3 weeks for the *Hevin*$^{-/-}$ and 4 weeks in 129SVE vs 4 weeks for the *Fmr1*$^{-/y}$ and 5 weeks in C57BL/6 (Fig. 6B). The differences between C57BL/6 and *Fmr1*$^{-/y}$ and between 129SVE and *Hevin*$^{-/-}$ were also significant at 3 weeks (Fig 6B). Once established, there were no significant differences in the magnitude of L-LTP between mouse strains or genotypes across time post-induction (Fig. 6C).

Fig. 7.

The magnitude of the naïve fEPSP did not predict the developmental onset of L-LTP.

The naïve fEPSP slopes were compared across experiments to test their potential effect in determining when L-LTP was first produced. In each of the three key age groups, the slices were divided as having no LTP at 3 hr or having L-LTP at 3 hr. No significant differences in the naïve

bioRxiv preprint first posted online Sep. 30, 2019; doi: http://dx.doi.org/10.1101/787192. The copyright holder for this preprint (which was not peer-reviewed) is the author/funder, who has granted bioRxiv a license to display the preprint in perpetuity. It is made available under a CC-BY-NC-ND 4.0 International license.

slopes were detected across strains, genotypes, or age groups (Fig. 7). Thus, the magnitude of the naïve responses did not determine the occurrence of L-LTP in these experiments.

Fig. 8

Age dependence of the augmentation of L-LTP.

Prior work in the rat hippocampus revealed that multiple time-separated episodes of TBS result in additional potentiation or augmentation of L-LTP. The timing of this effect is strain and age-related in the rat hippocampus (Bowden et al., 2012; Cao and Harris, 2012, 2014; Kramar et al., 2012; Manahan-Vaughan, 2000; Manahan-Vaughan and Schwegler, 2011). We tested whether a pair of 8T episodes spaced 180 min apart would augment L-LTP in mouse hippocampus, as it does in rat (Fig. 8A). Two criteria were set for augmentation. First, the initial potentiation was at least 120% of the naïve response at three hours post tetanus. Second, following the second 8T the fEPSP slope was elevated $\geq$10% above the initial L-LTP and lasted at least 70 minutes. Longer monitoring of responses in slices from developing animals could become unreliable after 11 hours *in vitro* so experiments were terminated by 9 hours (i.e., 3 hours recovery plus 6 hours of recording). To meet criterion 1, slices from the different mouse genotypes were compared in their respective Onset or After Onset age groups. The time course of L-LTP and augmentation of L-LTP is illustrated for all four genotypes (Fig. 8B-E). At the age of L-LTP Onset some slices from the *Fmr1*$^{-/y}$ mutant mice with threshold levels of initial L-LTP produced augmentation of L-LTP, whereas none of the other genotypes met the 10% augmentation criterion (Fig. 8C,F). After the age of L-LTP Onset all 4 genotypes produced augmentation of L-LTP (Fig. 8F). For the *Hevin*$^{-/-}$, slices from both 3 and 4 week old mice were technically in the After L-LTP Onset age group. However, slices from 4 week old *Hevin*$^{-/-}$ animals produced a more robust augmentation of L-LTP, while slices from 3 week old *Hevin*$^{-/-}$ animals produced less augmentation that did not reach the criterion (Fig. 8E,F). Hence, the *Hevin*$^{-/-}$ slices tested for augmentation were separated by age, with 3 weeks in the Onset group to illustrate the modest augmentation and 4 weeks in the After Onset group to illustrate the more robust augmentation (Fig. 8F).

Even after the onset age of L-LTP, some slices showed no initial L-LTP. In those slices, the second 8T also produced no potentiation and hence no augmentation (Fig. 8G). In fact, for slices without initial L-LTP in the C57BL/6 and *Hevin*$^{-/-}$ mice, the second 8T episode resulted in significant depression 45-70 minutes later (Fig. 8B,E,G). This depression could merely reflect the failure to reverse the ongoing decline in the fEPSP slope normally observed over time in slices from developing animals that fail to produce initial L-LTP.

Fig. 9

Multiple episodes of 8T do not enable L-LTP in slices initially lacking production of L-LTP.

Since two episodes of 8T produced no potentiation in slices lacking initial L-LTP, further testing was done varying the timing (90 vs 180 min intervals) and strength (8T vs 1T) of the episodes

bioRxiv preprint first posted online Sep. 30, 2019; doi: http://dx.doi.org/10.1101/787192. The copyright holder for this preprint (which was not peer-reviewed) is the author/funder, who has granted bioRxiv a license to display the preprint in perpetuity. It is made available under a CC-BY-NC-ND 4.0 International license.

(Fig. 9A). Four week old C57BL/6 mice were chosen as this age was at the onset when a single episode of 8T did not reliably produce L-LTP. When two episodes of 8T were spaced by 90 minutes or 180 minutes, STP was present initially for 1 hour but no additional STP was produced after the second 8T and the response dropped back to baseline or below by 3 hours (Fig. 9B,C). When the more gentle 1T episodes were spaced by 90 minutes, substantial STP was induced after both the first and the second 1T episodes; however, this potentiation did not last (Fig, 9D, E). If the 1T episodes were spaced by 180 minutes, the second episode produced much less STP than the first, and the potentiation also did not last (Fig. 9D, E). Thus, neither change in timing or strength produced reliable initial L-LTP nor augmentation of STP to produce L-LTP at the earlier developmental stage.

DISCUSSION

In this study, a strong 8T induction paradigm was used to discern the developmental onset age for STP lasting 1 hour and L-LTP lasting more than 3 hr in mouse hippocampus. Because these gene manipulations alter dendritic spines, four mouse strains were chosen: C57BL/6 and *Fmr1*$^{-/y}$ on the C57BL/6 background and 129SVE and *Hevin*$^{-/-}$ (*Sparcl1*$^{-/-}$) on the 129SVE background. In all four strains, STP onset was gradual and first occurred between P10-P28. Reliable L-LTP emerged in C57BL/6 and *Fmr1*$^{-/y}$ by P35 and in 129SVE and *Hevin*$^{-/-}$ by P28, namely 5 and 4 weeks old, respectively. Multiple 8T with sufficient inter-episode intervals augmented L-LTP but did not elevate STP to L-LTP in mouse hippocampus. Hence, unlike rat hippocampus, multiple episodes of 8T did not alter the onset age of L-LTP in any of these mouse strains. Prior work in rats revealed that dendritic spines first form at P12, coincidentally with the developmental onset age of reliable L-LTP (Cao and Harris, 2012; Kirov et al., 2004). In contrast, mature dendritic spines are present by P15 in C57BL/6 mouse hippocampus (Bilousova et al., 2009), well before the onset age of reliable L-LTP. These species differences suggest that dendritic spines may be necessary but not sufficient for L-LTP.

Developmental Regulation of LTP in Mice

In the past, two major induction protocols were tested in rat hippocampus: repeated tetanic stimulation at 100 Hz for one second and multiple versions of the TBS protocol. These approaches revealed age differences in the onset of L-LTP. In rat hippocampus, tetanic stimulation produced L-LTP P15 (Harris and Teyler, 1984; Jackson et al., 1993), while TBS produced L-LTP earlier at P12 (Cao and Harris, 2012). Since TBS was a more efficient paradigm, it was used here to investigate the onset ages for STP and L-LTP in mouse hippocampus. Like in rat (Abrahamsson et al., 2007, 2008; Cao and Harris, 2012), de-depression occurred prior to STP onset in all mouse strains. There were no differences between mouse strains in the developmental onset of STP, which showed a gradual progression in success rate becoming reliable by 4 weeks of age. Onset of L-LTP differed by strain, with 129SVE and *Hevin*$^{-/-}$ becoming reliable by 4 weeks and C57BL/6 and *Fmr1*$^{-/y}$ becoming reliable by 5 weeks. The starting slopes of the fEPSPs were similar across the genotypes and ages, hence these

bioRxiv preprint first posted online Sep. 30, 2019; doi: http://dx.doi.org/10.1101/787192. The copyright holder for this preprint (which was not peer-reviewed) is the author/funder, who has granted bioRxiv a license to display the preprint in perpetuity. It is made available under a CC-BY-NC-ND 4.0 International license.

differences in L-LTP onset ages were not explained by differences in the initial strength of activation used across ages in the mice.

Plasticity and Spines

In rats, experiments during early postnatal development suggest a good correlation between L-LTP onset and spine formation. In rat hippocampus, spines were first detected with confocal microscopy in DiI filled dendrites in acute slices at P10-12 with a dramatic increase in number occurring by P21 (Kirov et al., 2004). Reliable L-LTP production at P12 was coincident with the first appearance of dendritic spines. Initial 3D reconstructions in perfusion-fixed rat hippocampus show evidence for mature dendritic spines at P12, but not at P8 or P10 (Smith, 2019). Preliminary data from rat hippocampal slices showed that 90 minutes after the initial 8T, dendritic spines were not produced at P8 (Harris et al., 2012), contrasting with rat hippocampal slices at P10-11 where spines were produced 90 minutes after the initial 8T (Smith, 2019).

Confocal microscopy studies reveal a few mushroom spines by 9-12 days in organotypic slices from mouse hippocampus (Parnass et al., 2000). Similarly, at 14 days in organotypic slices from C57BL/6 and *Fmr1*$^{-/y}$ more than 40% of the protrusions were classified as mushroom spines, although less than 10% had mature heads with a diameter greater than 0.5 μm (Bilousova et al., 2009). Reconstructions from serial EM show mature spines by P24 in the C57BL/6 hippocampus (Nikonenko et al., 2013). Thus, the onset of L-LTP appears to be later than the onset of dendritic spines in mouse hippocampus, suggesting that spines may be necessary but not sufficient. Alternatively, the variance in L-LTP onset ages among individual mice may reflect variation in the maturation of dendritic spines, whereas in rats, the discrete onset age of L-LTP may reflect less variation in these factors between individuals. In which case, it would be necessary to test individual mice at young ages for coincidence of L-LTP and spinogenesis.

Developmental metaplasticity

Some patterns of stimulation have no direct effect on synaptic strength but instead modulate the subsequent expression of plasticity, a phenomenon known as metaplasticity (Abraham and Bear, 1996; Abraham and Tate, 1997; Young and Nguyen, 2005). Spaced learning produces longer memories than massed learning, and the efficacy of memory is dependent on the interval between episodes of learning (Ebbinghaus, 1885; Fields, 2005). Similarly, spacing episodes of plasticity induction is considered to be a good model for understanding the cellular mechanisms of spaced learning (Kramar et al., 2012; Lynch and Gall, 2013; Lynch et al., 2013). Regarding LTP, sufficient time must pass between the TBS episodes to augment LTP after a second episode of TBS. In adult rat, augmentation of LTP is first observed at 90 min spacing between episodes of 8T and prolonging the time between TBS episodes increases the probability of augmentation (Cao and Harris, 2014). The delay between episodes of TBS reflects the time needed to enlarge the synapses after the initial induction of LTP in adult rats (Bell et al., 2014). In adults, this synaptic enlargement is also homeostatically balanced by stalled spine outgrowth which reflects

bioRxiv preprint first posted online Sep. 30, 2019; doi: http://dx.doi.org/10.1101/787192. The copyright holder for this preprint (which was not peer-reviewed) is the author/funder, who has granted bioRxiv a license to display the preprint in perpetuity. It is made available under a CC-BY-NC-ND 4.0 International license.

the temporal dynamics of resource reallocation at different times after the induction of LTP (Bell et al., 2014; Bourne and Harris, 2007; Chirillo et al., 2019). Others have shown in adult rats that TBS-induced L-LTP and unsupervised learning enhance actin polymerization and growth via phosphorylation of cofilin, especially in large spines (Chen et al., 2007; Fedulov et al., 2007).

Patterns of augmentation of L-LTP are also developmentally regulated. In rats, a second episode of 8T delivered 90 min after the first produced L-LTP at P10-P11, but not at P8-P9. In the C57BL/6 mice, applying a second 8T episode 90 or 180 minutes after the first did not produce LTP even at 4 weeks of age when STP was induced in most slices. Instead, in mouse hippocampus, augmentation could be achieved only after initial L-LTP was reliably established for C57BL/6, 129SVE, and *Hevin*$^{-/-}$. Curiously, augmentation of L-LTP was observed earlier in *Fmr1*$^{-/y}$ mice in slices with initial L-LTP. These observations suggest that the development of L-LTP and metaplasticity is a process independent from STP and, unlike in rat hippocampus, STP in mouse hippocampus does not advance the maturation of synapses.

Implications for developmentally regulated brain disorders

Our data suggest that L-LTP and STP may influence developmentally regulated cognitive disorders. The onset of L-LTP was defined when 25-50% of slices produced L-LTP. The onset of L-LTP in *Fmr1*$^{-/y}$ at 4 weeks was delayed relative to the background C57BL/6 strain at 3 weeks. This pattern contrasted with the earlier onset age in *Hevin*$^{-/-}$ by 2 weeks, relative to its background 129SVE strain between 2-3 weeks. These findings are consistent with the known strain differences in the structural disruption of dendritic spines. *Fmr1*$^{-/y}$ neurons are characterized by an overproduction of underdeveloped spines that might not support the plasticity events (He and Portera-Cailliau, 2013). Treatment of neonatal *Fmr1*$^{-/y}$ mice with the antibiotic minocycline resulted in better learning outcomes and enhanced spine maturation (Bilousova et al., 2009). Furthermore, in adult *Fmr1*$^{-/y}$ mice (3-5 months old), spaced trials rescued learning deficits (Seese et al., 2014). In the developing *Fmr1*$^{-/y}$ mice, however, STP was not augmented to L-LTP upon spaced bouts of 8T in slices that had no initial L-LTP. Future work is needed to know whether the spaced learning effects were due to augmentation of L-LTP.

Hevin is required for the development of thalamocortical connectivity between P14-P25 (Risher et al., 2014). Moreover, when Hevin is absent, cortical dendritic spines show significant immaturity and a distinct refinement problem. In the second week of cortical development cortical spines often receive innervations from one cortical and one thalamic axon. By P25, these multiply innervated spines are refined to receive either a thalamocortical or intracortical synapse in wildtype (129SVE) mice. In the *Hevin*$^{-/-}$ mice this pruning effect does not occur uniformly and the ratio between thalamocortical and intracortical inputs is altered, retaining more of the intracortical synapses at the expense of thalamocortical connections. Furthermore application of Hevin protein to autoptic neurons results in a robust induction of NR2B containing NMDAR activity (Singh et al., 2016). The role of Hevin in refining hippocampal dendritic spines is unknown; however, its absence in *Hevin*$^{-/-}$ mice appears to promote the developmental onset of

bioRxiv preprint first posted online Sep. 30, 2019; doi: http://dx.doi.org/10.1101/787192. The copyright holder for this preprint (which was not peer-reviewed) is the author/funder, who has granted bioRxiv a license to display the preprint in perpetuity. It is made available under a CC-BY-NC-ND 4.0 International license.

L-LTP. Perhaps the lack of regulation of the NR2B subunit in the *Hevin*$^{-/-}$ mice stimulates the maturation of synapses at an earlier developmental stages.

Such striking differences are consistent with genetic analysis showing that almost half of the ~11K genes tested show differential expression between mice and rats in hippocampal dendrites, with much less divergence in the other tissues (Francis et al., 2014). There are also large differences between rat and mouse adult hippocampal neurogenesis, a process that is especially important for learning and memory (Lazarov and Hollands, 2016; Snyder et al., 2009). Rats had more adult-born, death-resistant neurons, and these neurons matured faster in rats than in mice. The young neurons showed a much higher contribution to fear learning tasks in rats than mice (Miller and Hen, 2015). These genetic and functional differences are consistent with rats having an earlier and more discrete onset age of L-LTP than mice. The absence of the discrete correlation between L-LTP onset and spine formation in mouse hippocampus further suggests that maturation of neurons and synapses is more gradual in mouse than rat hippocampus.

bioRxiv preprint first posted online Sep. 30, 2019; doi: http://dx.doi.org/10.1101/787192. The copyright holder for this preprint (which was not peer-reviewed) is the author/funder, who has granted bioRxiv a license to display the preprint in perpetuity. It is made available under a CC-BY-NC-ND 4.0 International license.

ADDITIONAL INFORMATION

Competing interests.

All authors declare no conflict of interests.

Author contributions.

The work has been conducted in the Center for Learning and Memory, Department of Neuroscience, the University of Texas at Austin. All authors qualify for authorship, and all those who qualify for authorship are listed. All authors approved the final version of the manuscript and agree to be accountable for all aspects of the work in ensuring that questions related to the accuracy or integrity of any part of the work are appropriately investigated and resolved.
OIO analyzed and interpreted the data, created the figures and drafted the paper; GC collected and analyzed the data; CE conceived and designed the work, provided the animals, and revised the paper; KMH conceived and designed the work, analyzed data, revised the paper, and obtained funding.

Funding.

This work was supported by National Institutes of Health Grants NS021184, NS033574, NS074644, MH-095980, MH-104319, the National Science Foundation (NSF) Grant 1707356 to K. M. Harris and the Texas Emerging Technologies Fund and NIH/NIDA R01 (DA031833) and NIH/NINDS R01-NS102237 to C.E.

Acknowledgements.

We thank Dr. Darrin Brager for providing the breeding pairs of *Fmr1*$^{-/y}$ mice, and Mr. Clay Smith and Ms. Amanda Heatherly for maintaining the mouse colony.

bioRxiv preprint first posted online Sep. 30, 2019; doi: http://dx.doi.org/10.1101/787192. The copyright holder for this preprint (which was not peer-reviewed) is the author/funder, who has granted bioRxiv a license to display the preprint in perpetuity. It is made available under a CC-BY-NC-ND 4.0 International license.

FIGURE LEGENDS

Figure 1: L-LTP was reliably produced by 5 weeks of age for (A) C57BL/6 and (B) *Fmr1*$^{-/y}$ mice.
(Top row) Electrode positions in hippocampal area CA1 and slice paradigm to test for L-LTP. Slices were recovered for 3 hr without stimulation. Then an I/O was done to determine half-maximal response, which was repeated at 2 min intervals to obtain the baseline responses. The 8T consisted of 8 trains at 30 second intervals with 10 bursts at 5 Hz of 4 pulses each at 100 Hz. Then the responses were monitored for 180 minutes and L-LTP was determined by averaging the response slope over the last 155-180 min (tan frame). (A1, B1) Before onset age of L-LTP: Hippocampus from animals of both genotypes that were less than 3 weeks old rarely produced LTP lasting 3 hrs. (A2) Onset age of L-LTP: By 3-4 weeks, about a third of the C57BL/6 and (B2) nearly half of the *Fmr1*$^{-/y}$ mice showed L-LTP lasting at least 3 hr. (A3, B3) After Onset age of L-LTP: By 5 weeks of age, well over half of the animals showed LTP lasting more than 3 hr for both genotypes. In time course plots and pie charts, the experiments with no potentiation (none) are colored black, those with STP lasting less than 1 hr (STP 1h) are colored gray, and those with LTP lasting 3 hr (LTP 3h) are colored red. Representative waveforms for pre-TBS baseline responses are colored gray, for 3 hr post-TBS are colored black for no potentiation and red for L-LTP at 3h. The pie charts show the relative fractions with the actual number of slices in each fraction for each age. The numbers of all animals and slices are also listed in Table 1.

Figure 2: **Week by week analysis of STP and L-LTP in the C57BL/6 (A1-A5) and *Fmr1*$^{-/y}$ (B1-B5) mice.** The same color and labeling schemes as in Figure 1.

Figure 3: LTP was reliably produced after 3 weeks of age for 129SVE (A1-3) and *Hevin*$^{-/-}$ (B1-3) mice. The same color and labeling schemes as in Figure 1.

Figure 4: Week by week analysis of 1 hr and 3 hr LTP in the 129SVE (A1-4) and *Hevin*$^{-/-}$ (B1-4) mice. The same color and labeling schemes as in Figure 1.

Figure 5: Demonstration that 8T is a robust induction paradigm for L-LTP for all strains and genotypes. Reducing the number of trains in the TBS paradigm from 8T to 1-4T resulted in the same magnitude and endurance of L-LTP in (A) C57BL/6 , (B) *Fmr1*$^{-/y}$, (C) 129SVE, and (D) *Hevin*$^{-/-}$. The slices were obtained from animals at After Onset ages for each genotype.

Figure 6: Differences among strains in the probability of L-LTP. The probability of STP (A) and L-LTP (B) by strain and genotype across postnatal age. The probabilities were calculated as the ratio of the number of successful STP or L-LTP experiments relative to the total number of experiments for each condition and age group. No significant differences were detected for STP. Significant differences were detected for the probability of L-LTP (B) at postnatal week 3 (χ^2 = 13.16, df = 3; **P=0.0043) and postnatal week 4 (χ^2 = 16, df = 3; **P=0.0012). 129SVE strain

bioRxiv preprint first posted online Sep. 30, 2019; doi: http://dx.doi.org/10.1101/787192. The copyright holder for this preprint (which was not peer-reviewed) is the author/funder, who has granted bioRxiv a license to display the preprint in perpetuity. It is made available under a CC-BY-NC-ND 4.0 International license.

had a significantly higher probability of L-LTP than C57BL/6 at 4 wks (χ^2 = 12, df = 3; ***P=0.0006). Within backgrounds, a significant difference was detected at 3 weeks between C57BL/6 and *Fmr1*$^{-/y}$ (χ^2 = 4.875, df = 1; *P=0.0272) and between 129SVE and *Hevin*$^{-/-}$ (χ^2 = 5.490, df = 1; *P=0.0191). All genotype pairs were equal at week 5. (C) The magnitude of fEPSP potentiation at different time periods post TBS did not differ significantly across strains or genotypes in the After Onset age groups for each strain or genotype.

Figure 7: Magnitude of starting naïve responses did not predict success of L-LTP across ages, strains, or genotypes. Slices in each age group lacking L-LTP (black dots, gray bars) or producing 3 hr L-LTP (red dots and bars). Age groups are indicated as Before, Onset, and After the onset of L-LTP for each genotype. No significant differences were detected across the genotypes or stages for the Before onset group, or for the Onset vs After L-LTP onset groups (2-way ANOVA, Interaction: F(7, 127) = 0.691 (P=0.680), Age: F(1, 127) = 0.0722 (P=0.789), Genotype: F(1, 127) = 1.57 (P=0.151)). All data are presented as mean ± s.e.m with individual slice values as dots. Only 3 slices showed L-LTP in the Before onset group, so these were not included in the statistical analyses.

Figure 8: A second episode of 8T separated in time augments the initial L-LTP. (A) Experimental schematic: Recovery, I/O, Baseline, and first 8T matched original experiments (see figure 1). Responses were monitored for 180 minutes after the first 8T, and a second 8T was delivered at 180 min (red arrowhead). The initial L-LTP was averaged over 155-180 min after the first 8T (orange frame). The effect of the second 8T was calculated 45-70 min later (black frame, 225-260 min after the first 8T). (B-E) Normalized fEPSP slope time course during the experiment plotted for (B) C57BL/6, (C) *Fmr1*$^{-/y}$, (D 129SVE, and € *Hevin*$^{-/-}$. Augmentation of L-LTP was calculated as the percentage difference between fEPSP slope after the second TBS (black frame) relative to that after the first TBS (orange frame). L-LTP was considered to have undergone augmentation if the difference was at least 10% (red dotted line). (F) Summary for the augmentation of LTP across genotypes at L-LTP Onset (C57BL/6: t=6.335, df=5, partial η^2 = 0.889, **P= 0.0014; *Fmr1*$^{-/y}$: t=4.646, df=5, partial η^2 = 0.812; *P= 0.0056; 129SVE: t=6.221, df=5, partial η^2 = 0.886, **P= 0.0016; *Hevin*$^{-/-}$: t=5.184, df=5, partial η^2 = 0.843, **P= 0.0035) and After Onset developmental stages in slices that expressed L-LTP. For *Hevin*$^{-/-}$ the Onset group includes slices from 3 week old animals, and the After L-LTP Onset group included slices from the 4 week old cohort. (G) Lack of augmentation in slices from 4 week old animals that did not express L-LTP after the first TBS, and two genotypes showed further significant decline (C57BL/6: t=12.11, df=5, partial η^2 = 0.967, ***P< 0.0001; *Hevin*$^{-/-}$: t=7.369, df=5, partial η^2 = 0.916, ***P= 0.0007).

Figure 9: Three episodes of 8T did not produce L-LTP in slices lacking initial L-LTP in 4 week old C57BL/6 mice. (A) Experimental schematic: Each slice was subjected to two identical TBS paradigms consisting of either 1 or 8 trains that were spaced by 90 min (1T light blue, 8T

bioRxiv preprint first posted online Sep. 30, 2019; doi: http://dx.doi.org/10.1101/787192. The copyright holder for this preprint (which was not peer-reviewed) is the author/funder, who has granted bioRxiv a license to display the preprint in perpetuity. It is made available under a CC-BY-NC-ND 4.0 International license.

pink arrows) or 180 min (1T navy, 8T red arrows). Initial L-LTP was calculated by averaging responses 60-85 min before the second 8T at 85 min (gray time frame) or 155-180 min for the 180 min 8T interval (orange time frame). The effect of the second 8T was calculated at 135-160 min for the 90 min interval (green time frame) or at 225-260 min for the 180 min interval (black time frame). (B) Summary of the mean changes in fEPSP slope normalized to the 30 min averaged baseline responses with 8T TBS episodes spaced 90 min (pink) or 180 min (red). (C) Quantification of the experiments at the representative time frames for the experiments in B. No significant differences were detected at any of the time points for the different separations in 8T. (D) Summary of the mean changes in fEPSP slope normalized to the 30 min of the averaged baseline responses with 1T TBS episodes spaced 90 min (blue) or 180 min (navy). (E) Quantification of the experiments at the representative time frames for the experiments in D. No significant differences were detected between the levels of potentiation at orange and black intervals (pre and post second 1T spaced 180 min after the first 1T, 1-way ANOVA, $F(3, 9) = 2.736$, $P = 0.267$). A significant difference was detected by 2-way RM ANOVA between 1T-90m-1T and 1T-180m-8T by TBS spacing factor ($F(1, 7) = 6.762$; $^{*}p=0.0354$).

Table 1: Total number of slices and animals in each strain and age group.

bioRxiv preprint first posted online Sep. 30, 2019; doi: http://dx.doi.org/10.1101/787192. The copyright holder for this preprint (which was not peer-reviewed) is the author/funder, who has granted bioRxiv a license to display the preprint in perpetuity. It is made available under a CC-BY-NC-ND 4.0 International license.

Bibliography:

The Dutch-Belgian Fragile X Consortium. 1994. Fmr1 knockout mice: a model to study fragile X mental retardation. Cell 78(1), 23-33.

Abraham, W.C., Bear, M.F., 1996. Metaplasticity: the plasticity of synaptic plasticity. Trends. Neurosci 19(4), 126-130.

Abraham, W.C., Huggett, A., 1997. Induction and reversal of long-term potentiation by repeated high-frequency stimulation in rat hippocampal slices. Hippocampus 7(2), 137-145.

Abraham, W.C., Tate, W.P., 1997. Metaplasticity: a new vista across the field of synaptic plasticity. Prog. Neurobiol 52(4), 303-323.

Abrahamsson, T., Gustafsson, B., Hanse, E., 2007. Reversible synaptic depression in developing rat CA3 CA1 synapses explained by a novel cycle of AMPA silencing-unsilencing. J. Neurophysiol 98(5), 2604-2611.

Abrahamsson, T., Gustafsson, B., Hanse, E., 2008. AMPA silencing is a prerequisite for developmental long-term potentiation in the hippocampal CA1 region. J. Neurophysiol 100(5), 2605-2614.

Barker, T.H., Framson, P., Puolakkainen, P.A., Reed, M., Funk, S.E., Sage, E.H., 2005. Matricellular homologs in the foreign body response: hevin suppresses inflammation, but hevin and SPARC together diminish angiogenesis. Am J Pathol 166(3), 923-933.

Bell, M.E., Bourne, J.N., Chirillo, M.A., Mendenhall, J.M., Kuwajima, M., Harris, K.M., 2014. Dynamics of nascent and active zone ultrastructure as synapses enlarge during long-term potentiation in mature hippocampus. J Comp Neurol 522(17), 3861-3884.

Bilousova, T.V., Dansie, L., Ngo, M., Aye, J., Charles, J.R., Ethell, D.W., Ethell, I.M., 2009. Minocycline promotes dendritic spine maturation and improves behavioural performance in the fragile X mouse model. J Med Genet 46(2), 94-102.

Bourne, J., Harris, K.M., 2007. Do thin spines learn to be mushroom spines that remember? Curr. Opin. Neurobiol 17(3), 381-386.

Bourne, J.N., Kirov, S.A., Sorra, K.E., Harris, K.M., 2007. Warmer preparation of hippocampal slices prevents synapse proliferation that might obscure LTP-related structural plasticity. Neuropharmacology 52(1), 55-59.

Bowden, J.B., Abraham, W.C., Harris, K.M., 2012. Differential effects of strain, circadian cycle, and stimulation pattern on LTP and concurrent LTD in the dentate gyrus of freely moving rats. Hippocampus 22(6), 1363-1370.

Cao, G., Harris, K.M., 2012. Developmental Regulation of the Late Phase of Long-Term Potentiation (L-LTP) and Metaplasticity in Hippocampal Area CA1 of the Rat. J Neurophysiol 107(3), 902-912.

bioRxiv preprint first posted online Sep. 30, 2019; doi: http://dx.doi.org/10.1101/787192. The copyright holder for this preprint (which was not peer-reviewed) is the author/funder, who has granted bioRxiv a license to display the preprint in perpetuity. It is made available under a CC-BY-NC-ND 4.0 International license.

Cao, G., Harris, K.M., 2014. Augmenting saturated LTP by broadly spaced episodes of theta-burst stimulation in hippocampal area CA1 of adult rats and mice. J Neurophysiol 112(8), 1916-1924.

Chen, L.Y., Rex, C.S., Casale, M.S., Gall, C.M., Lynch, G., 2007. Changes in synaptic morphology accompany actin signaling during LTP. J Neurosci 27(20), 5363-5372.

Chirillo, M.A., Waters, M.S., Lindsey, L.F., Bourne, J.N., Harris, K.M., 2019. Local resources of polyribosomes and SER promote synapse enlargement and spine clustering after long-term potentiation in adult rat hippocampus. Sci Rep 9(1), 3861.

Ebbinghaus, H., 1885. Über das Gedächnis: Untersuchungen zur experimentellen Psychologie. Veit & Co., Leipzig.

Ellenbroek, B., Youn, J., 2016. Rodent models in neuroscience research: is it a rat race? Dis Model Mech 9(10), 1079-1087.

Fedulov, V., Rex, C.S., Simmons, D.A., Palmer, L., Gall, C.M., Lynch, G., 2007. Evidence that long-term potentiation occurs within individual hippocampal synapses during learning. J Neurosci 27(30), 8031-8039.

Fiala, J.C., Feinberg, M., Popov, V., Harris, K.M., 1998. Synaptogenesis via dendritic filopodia in developing hippocampal area CA1. J. Neurosci 18(21), 8900-8911.

Fields, R.D., 2005. Making memories stick. Sci. Am 292(2), 75-81.

Francis, C., Natarajan, S., Lee, M.T., Khaladkar, M., Buckley, P.T., Sul, J.Y., Eberwine, J., Kim, J., 2014. Divergence of RNA localization between rat and mouse neurons reveals the potential for rapid brain evolution. BMC Genomics 15, 883.

Harris, K.M., Teyler, T.J., 1984. Developmental onset of long-term potentiation in area CA1 of the rat hippocampus. J. Physiol 346, 27-48.

Harris, K.M., Watson, D.J., Kuwajima, M., Cao, G., 2012. Shift in synapse structure and location advances the onset age of late-phase LTP. Society for Neuroscience, Society for Neuroscience Abstracts.

He, C.X., Portera-Cailliau, C., 2013. The trouble with spines in fragile X syndrome: density, maturity and plasticity. Neuroscience 251, 120-128.

Homberg, J.R., Wohr, M., Alenina, N., 2017. Comeback of the Rat in Biomedical Research. ACS Chem Neurosci 8(5), 900-903.

Jackson, P.S., Suppes, T., Harris, K.M., 1993. Stereotypical changes in the pattern and duration of long-term potentiation expressed at postnatal days 11 and 15 in the rat hippocampus. J. Neurophysiol 70(4), 1412-1419.

bioRxiv preprint first posted online Sep. 30, 2019; doi: http://dx.doi.org/10.1101/787192. The copyright holder for this preprint (which was not peer-reviewed) is the author/funder, who has granted bioRxiv a license to display the preprint in perpetuity. It is made available under a CC-BY-NC-ND 4.0 International license.

Kirov, S.A., Goddard, C.A., Harris, K.M., 2004. Age-dependence in the homeostatic upregulation of hippocampal dendritic spine number during blocked synaptic transmission. Neuropharmacology 47(5), 640-648.

Kramar, E.A., Babayan, A.H., Gavin, C.F., Cox, C.D., Jafari, M., Gall, C.M., Rumbaugh, G., Lynch, G., 2012. Synaptic evidence for the efficacy of spaced learning. Proc. Natl. Acad. Sci. U. S. A 109(13), 5121-5126.

Lazarov, O., Hollands, C., 2016. Hippocampal neurogenesis: Learning to remember. Prog Neurobiol 138-140, 1-18.

Lynch, G., Gall, C.M., 2013. Mechanism based approaches for rescuing and enhancing cognition. Front Neurosci 7, 143.

Lynch, G., Kramar, E.A., Babayan, A.H., Rumbaugh, G., Gall, C.M., 2013. Differences between synaptic plasticity thresholds result in new timing rules for maximizing long-term potentiation. Neuropharmacology 64, 27-36.

Manahan-Vaughan, D., 2000. Long-term depression in freely moving rats is dependent upon strain variation, induction protocol and behavioral state. Cereb. Cortex 10(5), 482-487.

Manahan-Vaughan, D., Schwegler, H., 2011. Strain-dependent variations in spatial learning and in hippocampal synaptic plasticity in the dentate gyrus of freely behaving rats. Front Behav. Neurosci 5, 7.

McKinnon, P.J., McLaughlin, S.K., Kapsetaki, M., Margolskee, R.F., 2000. Extracellular matrix-associated protein Sc1 is not essential for mouse development. Mol Cell Biol 20(2), 656-660.

Miller, B.R., Hen, R., 2015. The current state of the neurogenic theory of depression and anxiety. Curr Opin Neurobiol 30, 51-58.

Mongredien, R., Erdozain, A.M., Dumas, S., Cutando, L., Del Moral, A.N., Puighermanal, E., Rezai Amin, S., Giros, B., Valjent, E., Meana, J.J., Gautron, S., Callado, L.F., Fabre, V., Vialou, V., 2019. Cartography of hevin-expressing cells in the adult brain reveals prominent expression in astrocytes and parvalbumin neurons. Brain Struct Funct 224(3), 1219-1244.

Nikonenko, I., Nikonenko, A., Mendez, P., Michurina, T.V., Enikolopov, G., Muller, D., 2013. Nitric oxide mediates local activity-dependent excitatory synapse development. Proc. Natl. Acad. Sci. U. S. A 110(44), E4142-E4151.

Parnass, Z., Tashiro, A., Yuste, R., 2000. Analysis of spine morphological plasticity in developing hippocampal pyramidal neurons. Hippocampus 10(5), 561-568.

Pfeiffer, B.E., Huber, K.M., 2009. The state of synapses in fragile X syndrome. Neuroscientist 15(5), 549-567.

Risher, W.C., Patel, S., Kim, I.H., Uezu, A., Bhagat, S., Wilton, D.K., Pilaz, L.J., Singh Alvarado, J., Calhan, O.Y., Silver, D.L., Stevens, B., Calakos, N., Soderling, S.H., Eroglu, C., 2014. Astrocytes refine cortical connectivity at dendritic spines. Elife 3.

bioRxiv preprint first posted online Sep. 30, 2019; doi: http://dx.doi.org/10.1101/787192. The copyright holder for this preprint (which was not peer-reviewed) is the author/funder, who has granted bioRxiv a license to display the preprint in perpetuity. It is made available under a CC-BY-NC-ND 4.0 International license.

Seese, R.R., Wang, K., Yao, Y.Q., Lynch, G., Gall, C.M., 2014. Spaced training rescues memory and ERK1/2 signaling in fragile X syndrome model mice. Proc Natl Acad Sci U S A 111(47), 16907-16912.

Singh, S.K., Stogsdill, J.A., Pulimood, N.S., Dingsdale, H., Kim, Y.H., Pilaz, L.J., Kim, I.H., Manhaes, A.C., Rodrigues, W.S., Jr., Pamukcu, A., Enustun, E., Ertuz, Z., Scheiffele, P., Soderling, S.H., Silver, D.L., Ji, R.R., Medina, A.E., Eroglu, C., 2016. Astrocytes Assemble Thalamocortical Synapses by Bridging NRX1alpha and NL1 via Hevin. Cell 164(1-2), 183-196.

Smith, H., 2019. Shift in synapse structure and location advances the onset age of late-phase LTP, in: Haines, C., Cao, G., Ventura, S.L., Drake, M.H., Kuwajima, M., Harris, K.M. (Eds.). Society for Neuroscience, Society for Neuroscience Abstracts.

Snyder, J.S., Choe, J.S., Clifford, M.A., Jeurling, S.I., Hurley, P., Brown, A., Kamhi, J.F., Cameron, H.A., 2009. Adult-born hippocampal neurons are more numerous, faster maturing, and more involved in behavior in rats than in mice. J Neurosci 29(46), 14484-14495.

Xiao, M.Y., Wasling, P., Hanse, E., Gustafsson, B., 2004. Creation of AMPA-silent synapses in the neonatal hippocampus. Nat. Neurosci 7(3), 236-243.

Young, J.Z., Nguyen, P.V., 2005. Homosynaptic and heterosynaptic inhibition of synaptic tagging and capture of long-term potentiation by previous synaptic activity. J Neurosci 25(31), 7221-7231.

bioRxiv preprint first posted online Sep. 30, 2019; doi: http://dx.doi.org/10.1101/787192. The copyright holder for this preprint (which was not peer-reviewed) is the author/funder, who has granted bioRxiv a license to display the preprint in perpetuity. It is made available under a CC-BY-NC-ND 4.0 International license.

Fig 1

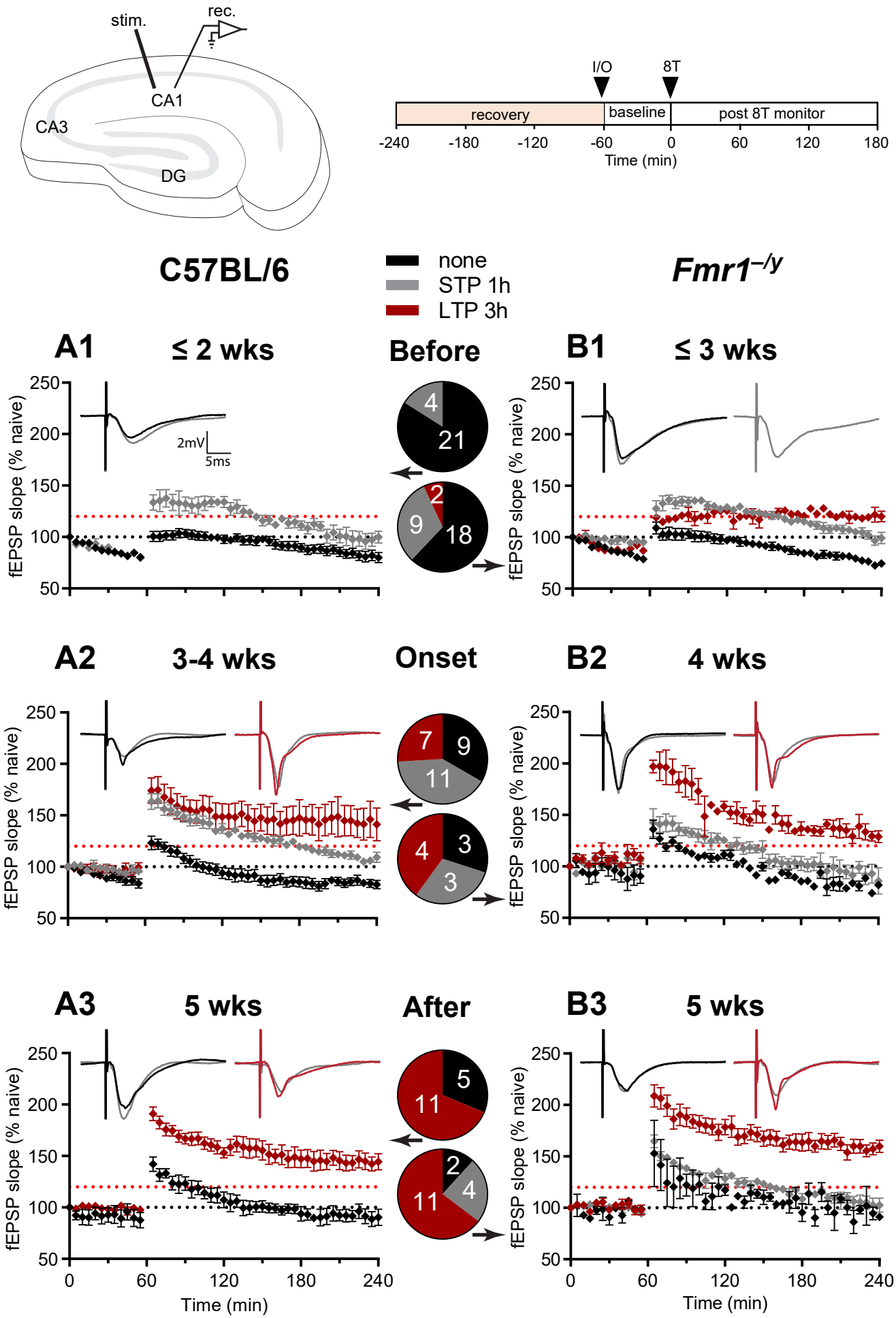

bioRxiv preprint first posted online Sep. 30, 2019; doi: http://dx.doi.org/10.1101/787192. The copyright holder for this preprint (which was not peer-reviewed) is the author/funder, who has granted bioRxiv a license to display the preprint in perpetuity. It is made available under a CC-BY-NC-ND 4.0 International license.

Fig 2

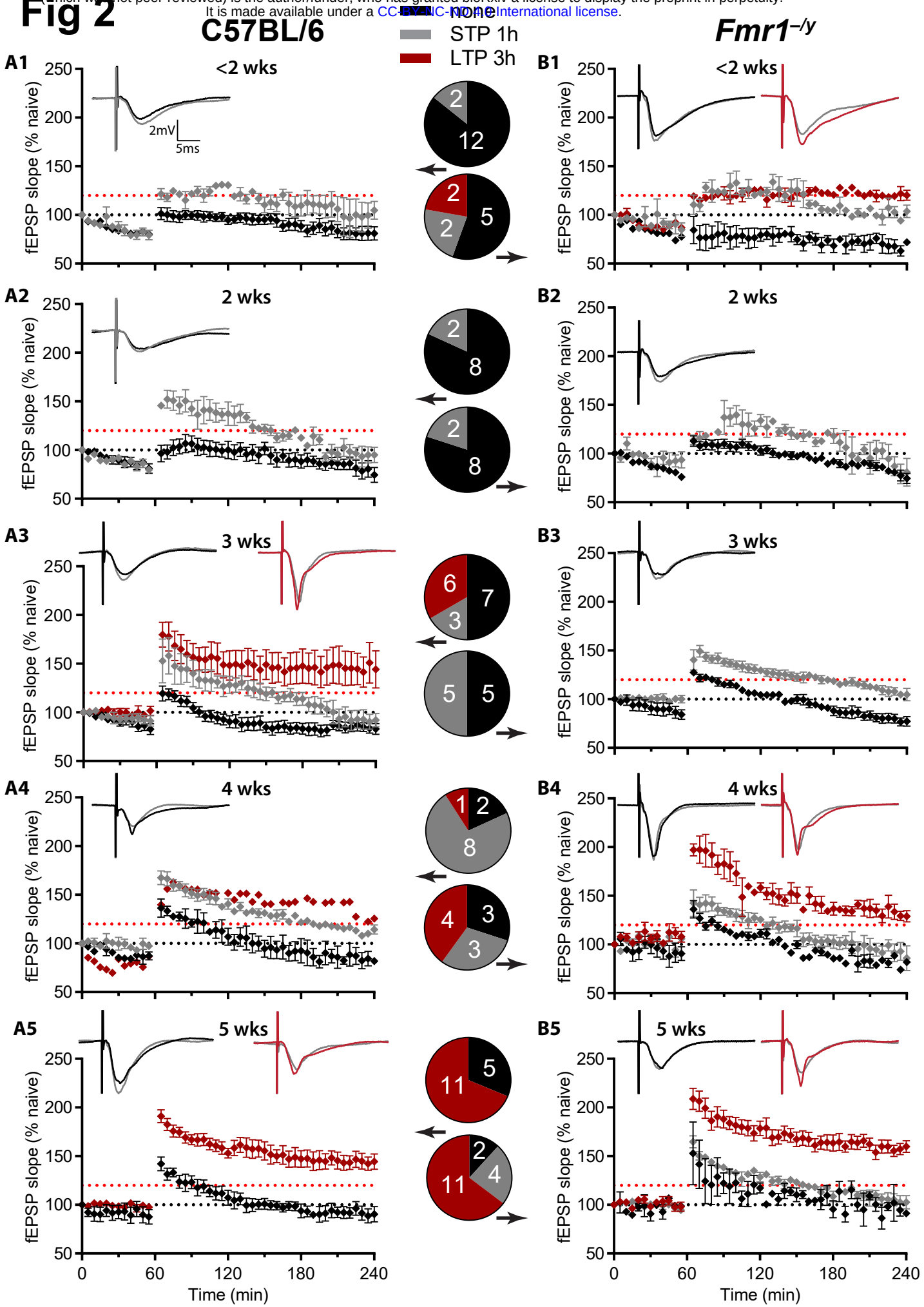

bioRxiv preprint first posted online Sep. 30, 2019; doi: http://dx.doi.org/10.1101/787192. The copyright holder for this preprint (which was not peer-reviewed) is the author/funder, who has granted bioRxiv a license to display the preprint in perpetuity. It is made available under a CC-BY-NC-ND 4.0 International license.

Fig 3

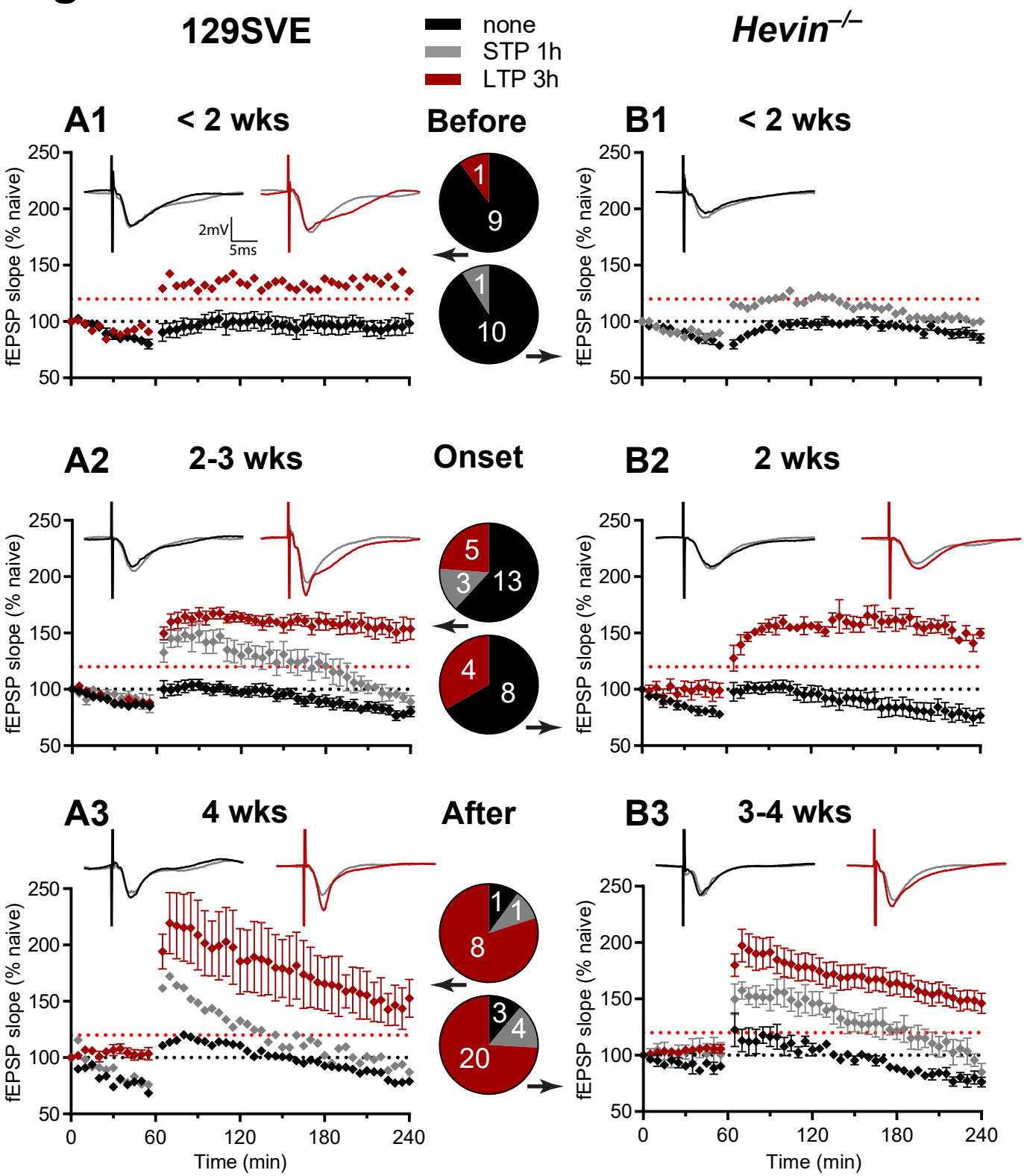

bioRxiv preprint first posted online Sep. 30, 2019; doi: http://dx.doi.org/10.1101/787192. The copyright holder for this preprint (which was not peer-reviewed) is the author/funder, who has granted bioRxiv a license to display the preprint in perpetuity. It is made available under a CC-BY-NC-ND 4.0 International license.

Fig 4

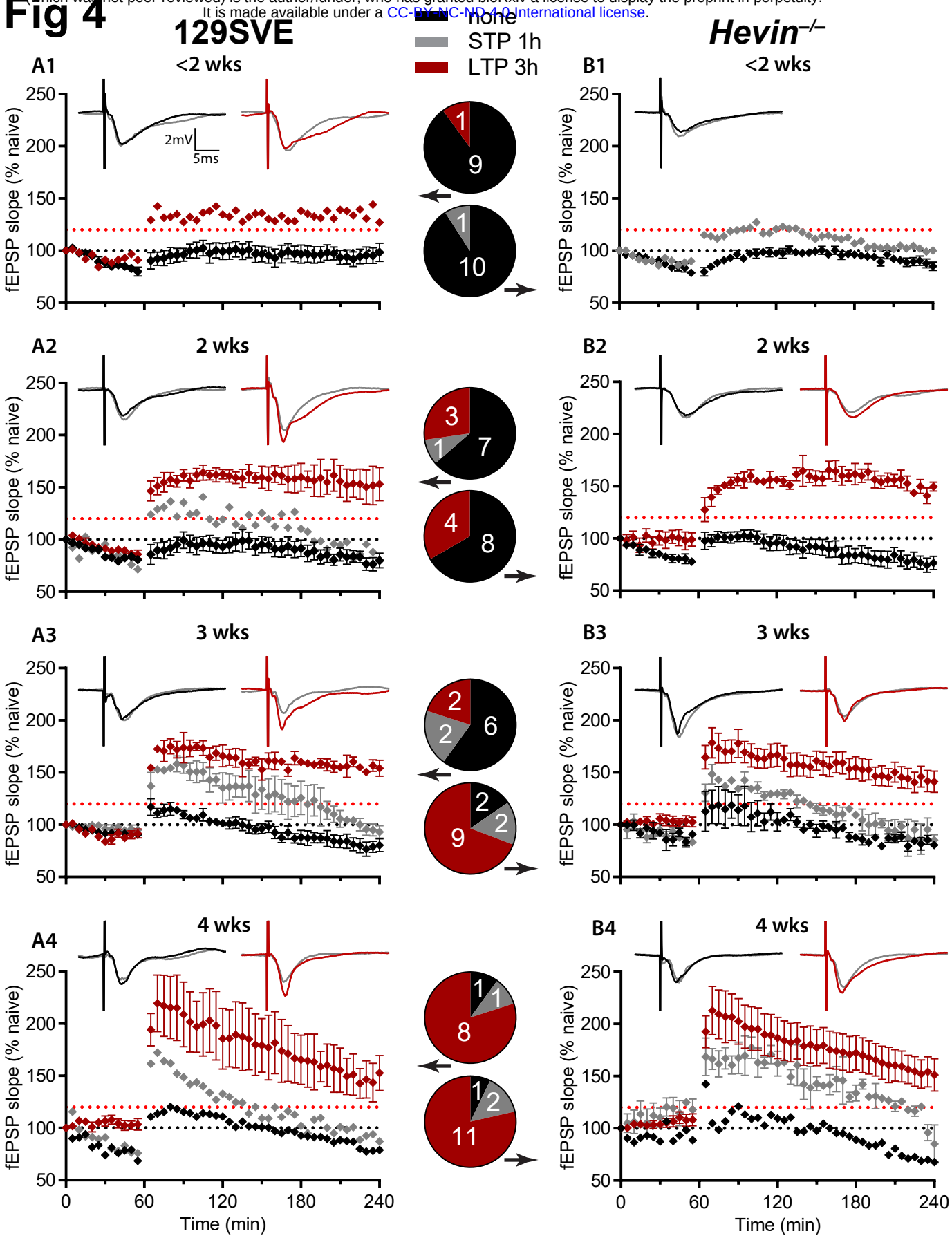

Fig 5

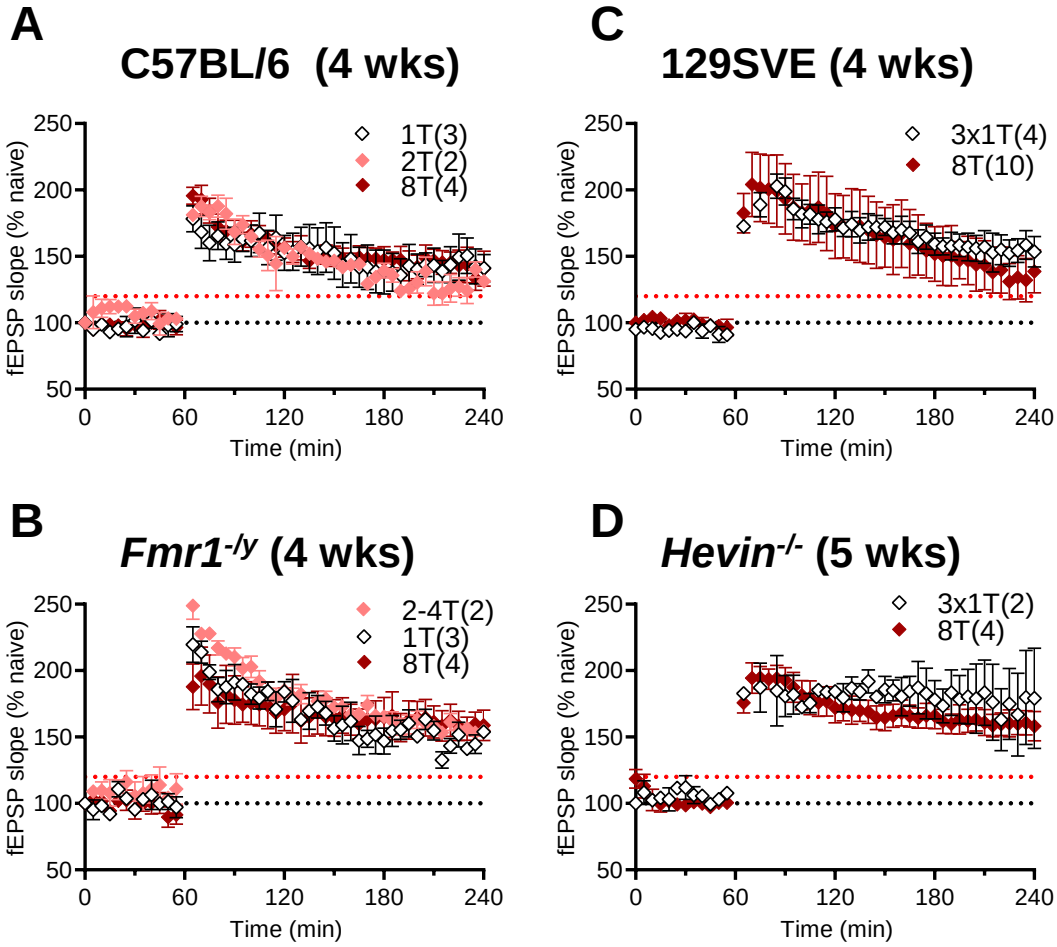
A
C57BL/6 (4 wks)
1T(3)
2T(2)
8T(4)
fEPSP slope (% naive)
250
200
150
100
50
0
60
120
180
240
Time (min)
C
129SVE (4 wks)
3x1T(4)
8T(10)
fEPSP slope (% naive)
Time (min)
B
Fmr1-/y (4 wks)
2-4T(2)
1T(3)
8T(4)
fEPSP slope (% naive)
Time (min)
D
Hevin-/- (5 wks)
3x1T(2)
8T(4)
fEPSP slope (% naive)
Time (min)

Fig 6

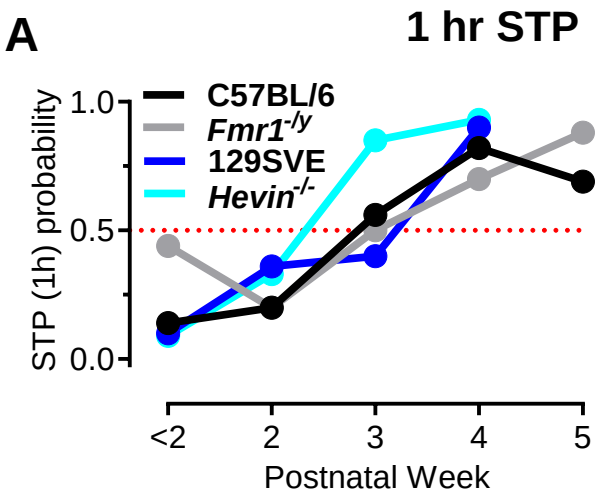
A
1 hr STP
C57BL/6
Fmr1-/y
129SVE
Hevin-/-
STP (1h) probability
1.0
0.5
0.0
<2
2
3
4
5
Postnatal Week

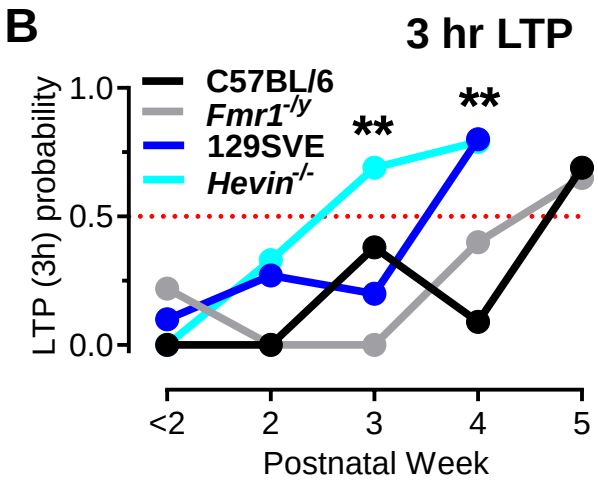
B
3 hr LTP
C57BL/6
Fmr1-/y
129SVE
Hevin-/-
**
**
LTP (3h) probability
1.0
0.5
0.0
<2
2
3
4
5
Postnatal Week

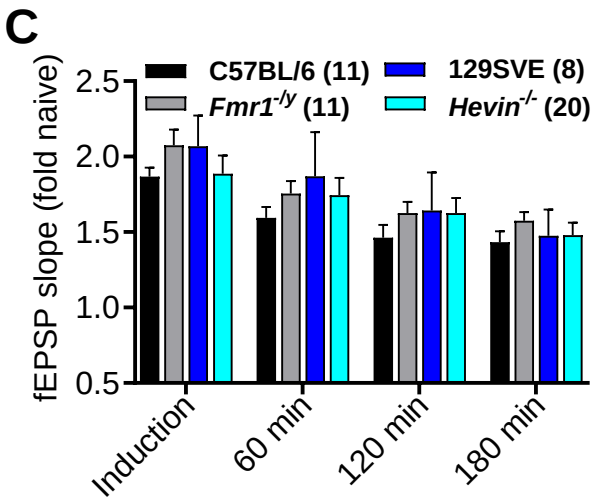
C
C57BL/6 (11)
129SVE (8)
Fmr1-/y (11)
Hevin-/- (20)
fEPSP slope (fold naive)
2.5
2.0
1.5
1.0
0.5
Induction
60 min
120 min
180 min

Fig. 7

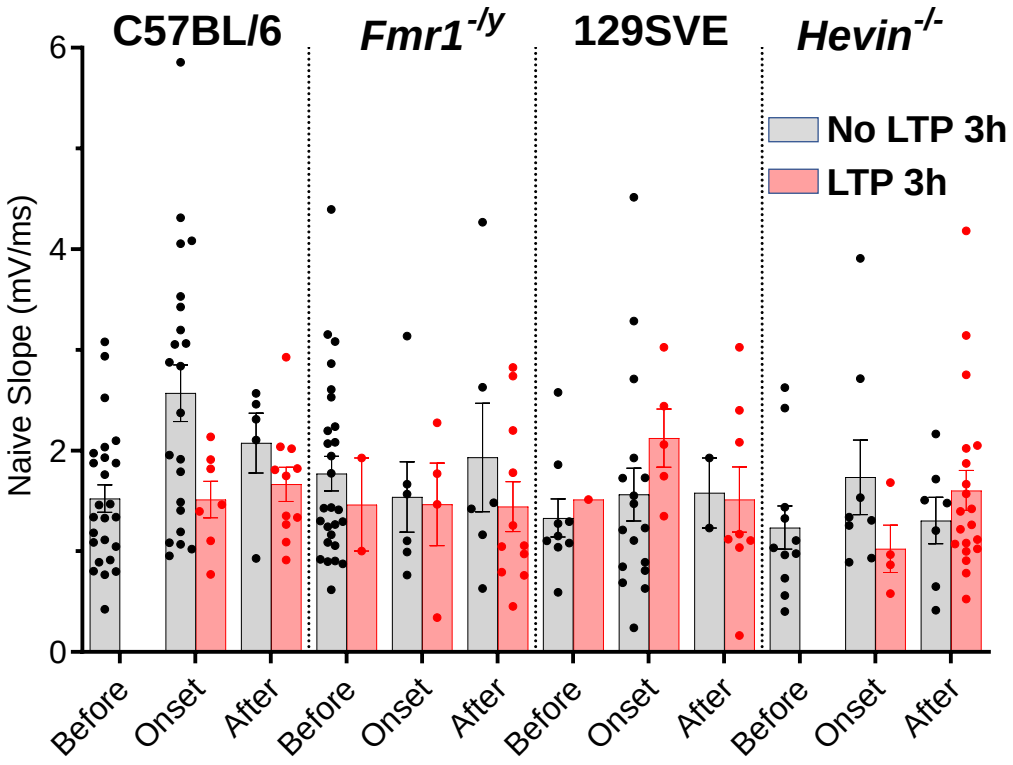
C57BL/6
Fmr1-/y
129SVE
Hevin-/-
No LTP 3h
LTP 3h
Naive Slope (mV/ms)
0
2
4
6
Before
Onset
After
Before
Onset
After
Before
Onset
After
Before
Onset
After

Fig. 8

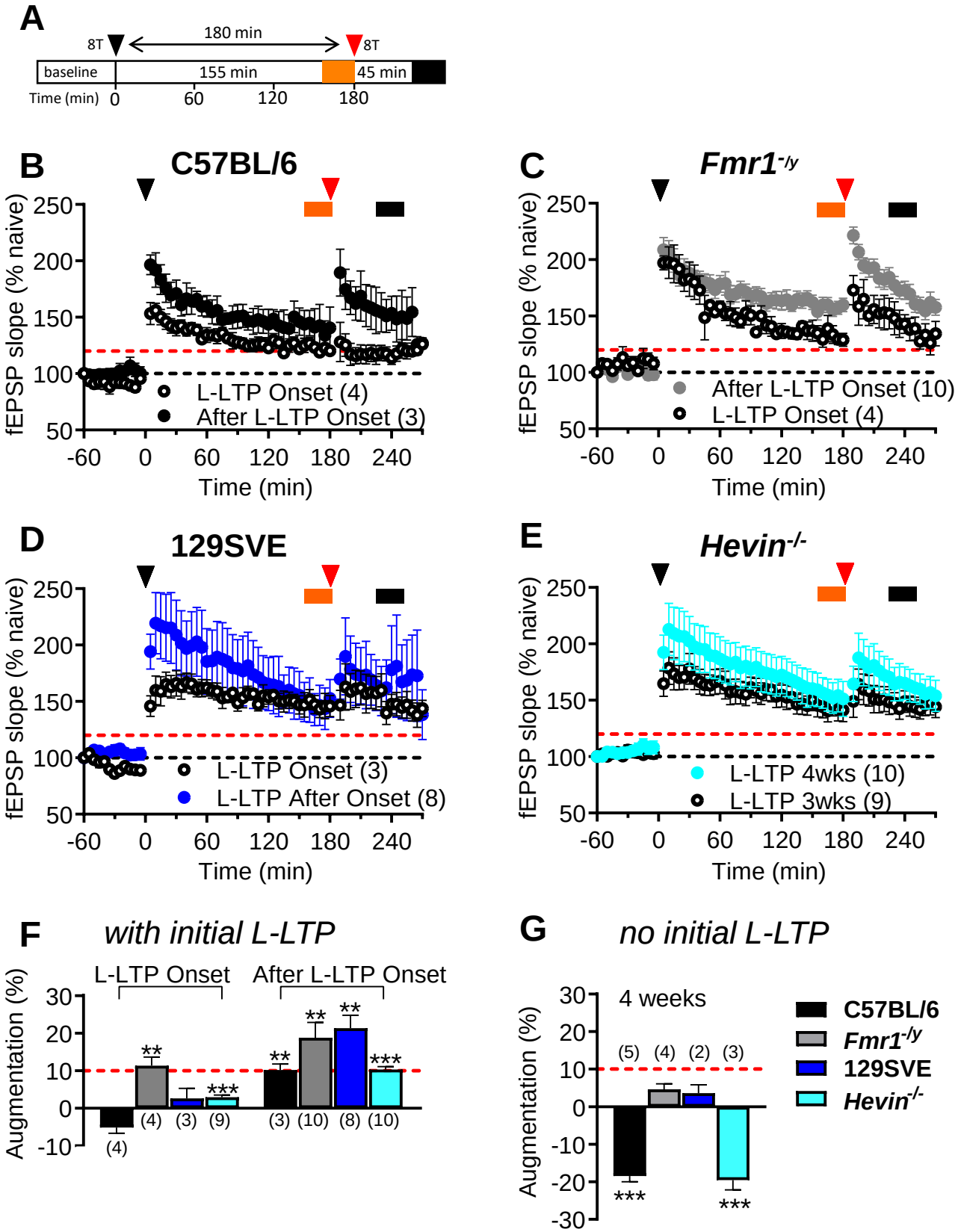
A
8T
180 min
8T
baseline
155 min
45 min
Time (min) 0 60 120 180
B
C57BL/6
fEPSP slope (% naive)
L-LTP Onset (4)
After L-LTP Onset (3)
Time (min)
C
Fmr1-/y
After L-LTP Onset (10)
L-LTP Onset (4)
D
129SVE
L-LTP Onset (3)
L-LTP After Onset (8)
E
Hevin-/-
L-LTP 4wks (10)
L-LTP 3wks (9)
F
with initial L-LTP
L-LTP Onset
After L-LTP Onset
Augmentation (%)
G
no initial L-LTP
4 weeks
C57BL/6
Fmr1-/y
129SVE
Hevin-/-

Fig. 9

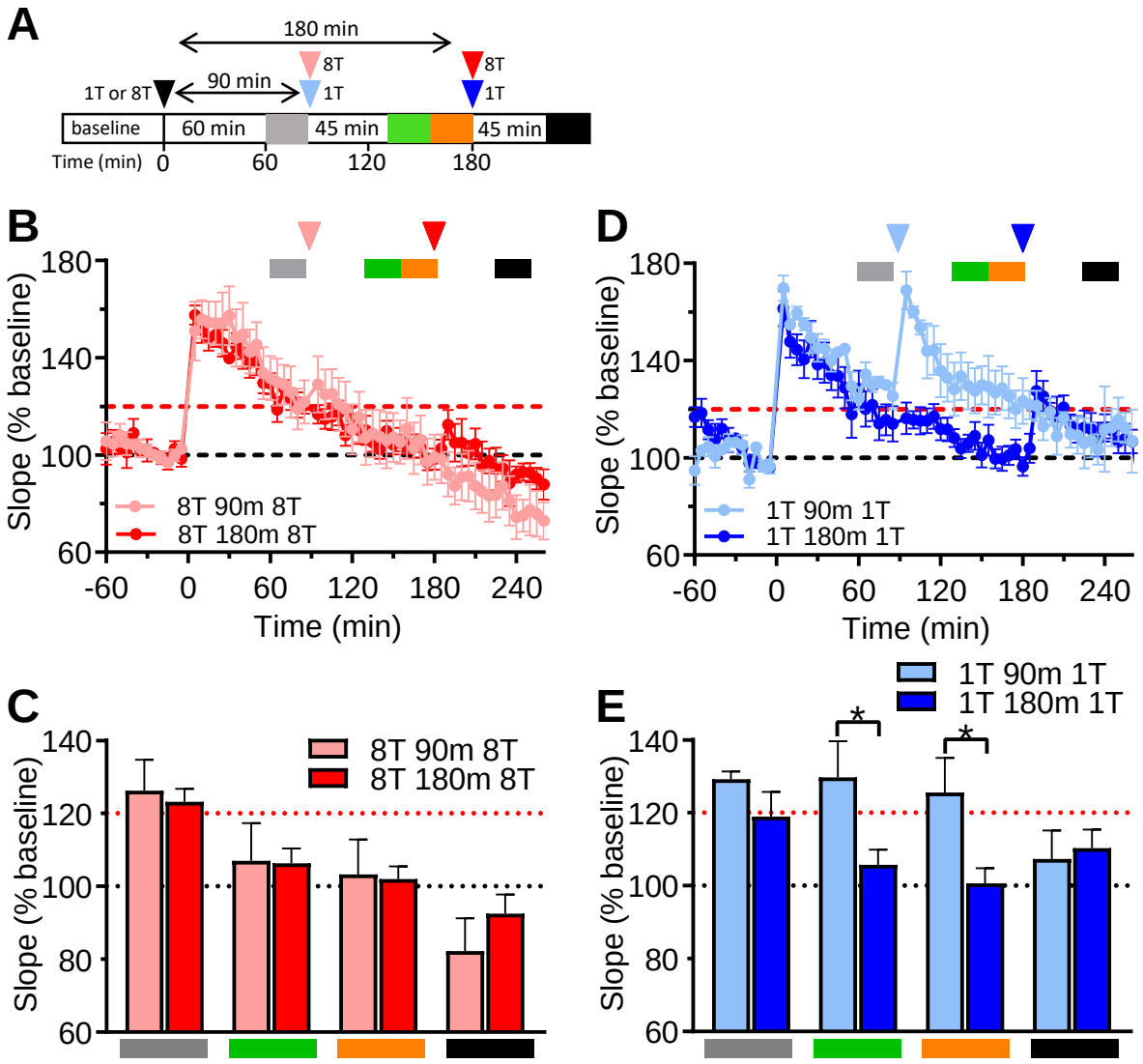
A
180 min
8T
8T
1T or 8T
90 min
1T
1T
baseline
60 min
45 min
45 min
Time (min)
0
60
120
180
B
Slope (% baseline)
180
140
100
60
8T 90m 8T
8T 180m 8T
-60
0
60
120
180
240
Time (min)
D
Slope (% baseline)
180
140
100
60
1T 90m 1T
1T 180m 1T
-60
0
60
120
180
240
Time (min)
C
Slope (% baseline)
140
120
100
80
60
8T 90m 8T
8T 180m 8T
E
1T 90m 1T
1T 180m 1T
Slope (% baseline)
140
120
100
80
60
*
*

Table 1

animals					
	<2wks	2wks	3wks	4wks	5wks
C57BL/6	8	7	10	8	6
Fmr1$^{-/y}$	6	4	6	4	7
129SVE	6	6	6	6	
Hevin$^{-/-}$ *(Sparcl1*$^{-/-}$*)*	5	5	6	7	
slices					
	<2wks	2wks	3wks	4wks	5wks
C57BL/6	14	11	18	11	16
Fmr1$^{-/y}$	9	10	10	10	17
129SVE	10	11	10	10	
Hevin$^{-/-}$ *(Sparcl1*$^{-/-}$*)*	11	12	13	14	